

# Generalization of the reaction-diffusion, the Swift-Hohenberg and the Kuramoto-Sivashinsky equation and effects of finite propagation speeds

Axel Hutt<sup>\*†</sup>

*Humboldt University at Berlin, Institute of Physics,  
Newtonstr. 15, 12489 Berlin, Germany*

(Dated: December 2, 2024)

## Abstract

The work proposes and studies a one-dimensional model, which involves nonlocal interactions and finite propagation speed. It shows that the general reaction-diffusion equation, the Swift-Hohenberg equation and the general Kuramoto-Sivashinsky equation represent special cases of the proposed model for limited spatial interaction ranges and for infinite propagation speeds. After a detailed validity study on the generalization conditions, the three equations are extended to involve finite propagation speeds. Moreover linear stability studies of the extended equations reveal critical propagation speeds and novel types of instabilities in all three equations. In addition, an extended diffusion equation is derived and studied in some detail with respect to finite propagation speeds. The extended model allows for the explanation of recent experimental results on non-Fourier heat conduction in non-homogeneous material.

PACS numbers: 02.30.Rz, 66.10.Cb, 02.30.Ks

---

<sup>\*</sup> Present address: Department of Physics, University of Ottawa, 150 Louis Pasteur, Ottawa, Ontario, K1N-6N5, Canada

<sup>†</sup> Electronic address: ahutt@uottawa.ca

## I. INTRODUCTION

The propagation of activity in spatially extended systems has attracted much attention in the last centuries, starting from celestial mechanics in the sixteenth century to the activity propagation in complex physical, chemical or biological systems [1, 2] in the last decades. In such systems the communication between the system subunits plays a decisive role. These subunits may be coupled locally to their next neighbors or may reveal longer-distance connections. In the latter case, the finite speed of interactions, i.e. the finite propagation speed, may yield temporal delays which affect the space-time dynamics of the system. Such effects have been found in several systems, e.g. in neural networks [3, 4, 5, 6], quantum devices [7], porous and non-homogeneous media [8, 9] and electronic circuits [10, 11] as the internet or computational networks.

In order to describe spatial systems mathematically, partial differential equations (PDE) have been applied widely. However, most PDE models neglect effects caused by finite propagation speeds in the system. To consider these effects in PDE models, various approaches have been followed as, e.g. the introduction of additional temporal derivatives [12] or temporal constant delays [13]. However, propagation delays depend on the distance between two locations and thus represent space-dependant delays. In contrast to the PDE formulation, a natural way to consider these delays are integral-differential equations (IDE) which sum up all activity in a spatial domain and easily consider propagation delay, see e.g. [14, 15]. Moreover, the strong connection between PDE and IDE models is well-known [16]. The present work proposes a novel IDE model involving finite propagation delays which generalizes well-studied PDE models in one spatial dimension, namely the reaction-diffusion models, the Swift-Hohenberg model and the Kuramoto-Sivashinsky model. Reaction-diffusion models allow for the mathematical description of diverse spatio-temporal phenomena, e.g. as heat propagation or phase transitions in solids [17, 18], chemical reactions in fluids [19, 20] or the pattern formation in biological systems [2, 16]. Moreover the Swift-Hohenberg equation represents the amplitude equation derived from the Rayleigh-Benard model at Rayleigh numbers near the onset of hydrodynamic convection [21], while it has been formulated and studied in solid state physics as well [22, 23]. Further, the Kuramoto-Sivashinsky equation [20, 24] allows for the study of various phenomena in fluids and solids as e.g. the phase turbulence in fluids [25], the thermal diffusive instabilities of flame fronts [26], the

directional solidification in alloys [27] or the interface instability during the application of industrial beam cutting techniques [28]. Additionally re-calling the mathematical description of neuronal populations by IDEs, the proposed model represents a generic pattern forming model with a vast range of possible applications.

In addition to the generalization described above, the novel IDE model allows for the extension of PDE models in order to consider propagation delay effects. The present work shows that the results obtained in IDE models involving finite propagation speeds can be applied easily to PDE models. Hence this work extends previous studies [29, 30] as it clearly distinguishes local dynamics from nonlocal spatial interactions and elicits the strong connection between well-known PDE-models of pattern forming systems and the IDE models in neural field theory [31, 32, 33]. We derive novel extensions of the diffusion equation, the Swift-Hohenberg equation and the Kuramoto-Sivashinsky equation now involving finite propagation speeds. These extensions are important if the speed of the propagating activity in the system approaches the propagation speed of the system. Such ultra-fast phenomena have been observed experimentally in solids [34, 35], in plasma [36] and on solid and fluid surfaces [37, 38].

The present work is structured as follows. Section II introduces the integral-differential equation model and elicits its formal relation to partial differential equations. Then the subsequent section shows the reduction procedure to the PDE models and investigates the validity of that reduction. Eventually section IV studies the linear behavior of three specific models and examines their dependence on the finite propagation speed, while the last section closes the work by a brief discussion of the obtained results.

## II. THE GENERAL MODEL

The present work considers the general evolution equation

$$\begin{aligned} \hat{T}V(x, t) &= h(V(x, t)) \\ &+ \int_{\Omega} K(x - y) f(V(y, t - T(x - y))) \\ &+ L(x - y) g(V(y, t - T(x - y))) \, dy \end{aligned} \quad (1)$$

with the scalar field variable  $V(x, t)$ , the propagation delay  $T(x - y) = |x - y|/c$  with the propagation speed  $c$  and the spatial domain  $\Omega$  which is assumed being finite but large.

Further the operator  $\hat{T} = \hat{T}(d/dt)$  defines the temporal dynamics with  $\hat{T}(0) = 1$ ,  $K(x)$ ,  $L(x)$  represent the probability densities of spatial interactions, while  $h$ ,  $f$  and  $g$  are functionals subject to the field variable  $V$ . Here the term  $h$  accounts for (non-)linear self-interactions while the two integrals in Eq. (1) represent two types of interactions, e.g. activation and inhibition or short and long-range interaction. We point out that Eq. (1) extends a previous IDE model [29] by considering local interactions and thus renders the model more realistic for physical systems. As we show in the subsequent section, this extension proves to be very powerful.

Some previous studies remarked that IDEs generalize partial differential equations [16, 29]. In this context the central equation is

$$\int_{-\infty}^{\infty} dy K(x-y) S(V(y)) = \sum_{n=0}^{\infty} (-1)^n K_n \frac{\partial^n S(V(x))}{\partial x^n} \quad (2)$$

with a nonlinear functional  $S$  and the kernel moments  $K_n = \int d\eta K(\eta) \eta^n / n!$   $\forall n \in \mathbf{N}_0$ . The expansion (2) represents an order expansion of spatial interactions whose order  $n$  indicates the spatial interaction range. Hence  $K_n$  represent the contribution of spatial interactions of order  $n$ . Typically local or short-range PDE models involve spatial derivatives of up to second order, while PDE models with spatial derivatives of up to fourth order involve non-local or long-range interactions. The expansion (2) extends this classification to spatial derivatives of arbitrary order.

### III. REDUCTION TO SPECIFIC MODELS

This section shows that Eq. (1) generalizes reaction-diffusion systems, the Swift-Hohenberg equation and the Kuramoto-Sivashinsky equation in one-dimensional spatial systems. Since these equations assume an infinite propagation speed in the system, we set  $T(x-y) = 0$ .

#### A. Reaction-diffusion equations

First let us focus on reaction-diffusion models. Here the terms in (1) are chosen as  $\hat{T} = \partial/\partial t$ ,  $g(V) = 0$  and  $f(V) = f_1 V$ . Further, the kernel  $K(x)$  is symmetric, i.e.  $K_{2n+1} = 0$ , and exhibits short-ranged spatial interactions with  $K_n \rightarrow 0$  for  $n > 2$ . Then the application

of Eq. (2) yields

$$\frac{\partial V(x, t)}{\partial t} = \bar{h}(V(x, t)) + D \frac{\partial^2}{\partial x^2} V(x, t) \quad (3)$$

with  $\bar{h}(V) = h(V) + K_0 f_1 V$  and  $D = K_2 f_1$ . This reaction-diffusion equation [20] accounts for (non-)linear self-interactions represented by  $\bar{h}(V)$  and considers local diffusive interactions with diffusion constant  $D$ . Hence, reaction-diffusion systems neglect spatial interactions of order  $n \geq 4$ .

### B. Swift-Hohenberg equation

To obtain the Swift-Hohenberg equation, the terms in (1) are chosen as  $\hat{T} = \partial/\partial t$ ,  $h(V) = aV - bV^3$ ,  $g(V) = 0$ ,  $f(V) = f_1 V$ ,  $f_1 < 0$ , the kernel  $K(x)$  is symmetric and now exhibits longer-ranged spatial interactions, i.e.  $K_n \rightarrow 0$  for  $n > 4$ . The subsequent application of Eq. (2) yields

$$\begin{aligned} \frac{\partial V(x, t)}{\partial t} &= aV(x, t) - bV^3(x, t) + K_0 f_1 V(x, t) \\ &\quad + K_2 f_1 \frac{\partial^2}{\partial x^2} V(x, t) + K_4 f_1 \frac{\partial^4}{\partial x^4} V(x, t) \end{aligned}$$

By choosing  $b = -K_2^2 |f_1| / 4K_4 > 0$  and re-scaling time and space according to  $t \rightarrow (-4K_4/K_2^2 |f_1|)t$  and  $x \rightarrow \sqrt{2K_4/K_2}x$  respectively, we find

$$\frac{\partial V(x, t)}{\partial t} = \varepsilon V(x, t) - V^3(x, t) - \left(1 + \frac{\partial^2}{\partial x^2}\right)^2 V(x, t) \quad (4)$$

with  $\varepsilon = -4K_4 a / K_2^2 |f_1| - 4K_4 K_0 / K_2^2 + 1$ . This equation is called Swift-Hohenberg equation [20]. Hence, systems obeying the Swift-Hohenberg equation neglect spatial interactions of order  $n \geq 6$ .

### C. Kuramoto-Sivashinsky equation

At last let us focus on the Kuramoto-Sivashinsky equation. Here, the terms in Eq. (1) are chosen as  $\hat{T} = \partial/\partial t$ ,  $g(V) = g_1 V$ ,  $f(V) = f_2 V^2$  with  $g_1, f_2 < 0$ . Now the kernel  $K(x)$  is non-symmetric and short-ranged, i.e.  $K_n \rightarrow 0$ ,  $n > 1$  while the kernel  $L(x)$  is chosen symmetric. Hence the corresponding kernel moments obey  $L_{2n+1} = 0$  and  $L(x)$  describes

long-range interaction with  $L_n \rightarrow 0, n > 4$ . Then the application of Eq. (2) leads to

$$\begin{aligned}\frac{\partial V(x, t)}{\partial t} &= (L_0 g_1 - h_0) V(x, t) + L_2 g_1 \frac{\partial^2}{\partial x^2} V(x, t) \\ &\quad + L_4 g_1 \frac{\partial^4}{\partial x^4} V(x, t) + 2K_1 f_2 V \frac{\partial V}{\partial x}\end{aligned}$$

while  $h(V)$  has been chosen as  $h(V) = -K_0 f_2 V^2 - h_0 V, h_0 \geq 0$ . Finally the re-scaling  $t \rightarrow (L_4/L_2^2|g_1|)t$  and  $x \rightarrow \sqrt{L_4/L_2}x$  yields

$$\begin{aligned}\frac{\partial V(x, t)}{\partial t} &= -\eta V - \frac{\partial^2}{\partial x^2} V(x, t) - \frac{\partial^4}{\partial x^4} V(x, t) - V \frac{\partial V}{\partial x}\end{aligned}\tag{5}$$

with  $\eta = |g_1|L_0 + h_0$  and the additional condition  $f_2 = L_2 \sqrt{L_2/L_4}/2K_1|g_1|$ . Equation (5) is called generalized Kuramoto-Sivashinsky equation [20] and  $\eta = 0$  represents the original Kuramoto-Sivashinsky equation. Hence systems obeying the Kuramoto-Sivashinsky equation involve symmetric spatial interactions up to order  $O(\sigma^5)$  and non-symmetric spatial interactions of order  $O(\sigma)$ . It is interesting to note that this model includes both non-symmetric and symmetric spatial interactions while the reaction-diffusion equation and the Swift-Hohenberg equation involve symmetric spatial interactions only.

#### D. Validity study

After the previous examinations, the question arises which specific kernel functions may fulfill the appropriate conditions in the three models. To this end, we apply the Fourier transform to the nonlinear function  $S(V(x))$  in (2) and obtain the spatial mode expansion

$$\int_{-\infty}^{\infty} dy K(x - y) S(V(y, t)) = \int_{-\infty}^{\infty} dk \tilde{S}(k, t) e^{ikx} \sum_{n=0}^{\infty} f_n(k)\tag{6}$$

with the sequence  $f_n(k) = (-ik)^n K_n$ . In the following, we abbreviate  $f_n = f_n(k)$  for convenience. As we will see later,  $f_n(k)$  represents the contribution of interactions at order  $n$  to the spatial modes of the system.

To obtain convergence of the series expansion in (2), the ratio of subsequent sequence terms  $|f_n|$  has to be smaller than unity. This means this condition reads  $|f_{n+2}|/|f_n| < 1$  for  $n$  even and  $|f_{n+1}|/|f_n| < 1$  for all  $n$  for symmetric and non-symmetric kernels, respectively.

To be more specific let us focus on a specific symmetric kernel function. Since the kernel represents the probability density function of the spatial interactions between two locations, the central limit theorem supports the choice of the Gauss function  $K(x) = \exp(-x^2/2\sigma^2)/\sqrt{2\pi}\sigma$  with the spatial range constant  $\sigma$ . Then the previous convergence condition leads to  $\sigma^2 < (n+2)/k^2, n = 2, 4, 6, \dots$ . If there is a maximum spatial frequency  $|k_m|$ , i.e. the Fourier transform  $\tilde{S}(|k|)$  is negligible for  $|k| > |k_m|$ , then the spatial interaction range  $\sigma$  is limited from above by  $\sqrt{n+2}/|k_m|$ . Subsequently, the spatial interaction range  $\sigma$  is delimited to the interval  $0 < \sigma^2 < 1/k_m^2$  which guarantees the Taylor expansion convergence in (2). We point out that the limitation to spatial modes is present in various physical systems. For instance, spatial systems near a phase transition exhibit a hierarchy of time scales of spatial modes with corresponding prominent spatial frequencies. In this case the time evolution of the Fourier transforms  $\tilde{S}(k, t)$  at spatial frequencies far from the prominent ones are negligible and the prominent frequencies define the maximum spatial frequency  $|k_m|$ . However, if there is no maximum spatial frequency, i.e.  $|k_m| \rightarrow \infty$ , it is  $\sigma \rightarrow 0$  and the convergence condition yields  $K(x) \rightarrow \delta(x)$ . Hence for an unlimited range of spatial frequencies, the expansion (2) is valid for local interactions only and  $K_n \rightarrow 0$  for  $n > 0$ .

Now let us interpret the latter results. It turns out that the convergence condition for Gaussian kernels leads to the dependence of the maximum spatial range on the interaction order  $n$ . For instance if the expansion in Eq. (2) approximates local interactions but no higher orders of nonlocality (cf. the previous discussion of the reaction-diffusion equation), it is  $|K_{n+2}/K_n| \ll 1$  for  $n = 2, 4, \dots$  and, subsequently,  $\sigma^2 < (2+2)/k^2 = 4/k^2$ . Hence, a maximum spatial frequency  $|k_m|$  yields the validity condition  $0 < \sigma^2 < 4/k_m^2$ . In case of spatial interactions at higher orders of nonlocality (cf. the previous discussion of the Swift-Hohenberg and the Kuramoto-Sivashinsky equation), it is  $|K_{n+2}/K_n| \ll 1$  for  $n = 4, 6, \dots$ . This means that the validity condition now reads  $0 < \sigma^2 < (4+2)/k_m^2 = 6/k_m^2$ . Thus the spatial interaction range  $\sigma$  may be larger than in the diffusion model.

Since the Kuramoto-Sivashinsky equation involves non-symmetric interactions, let us also examine briefly the kernel function  $K(x) = \delta(x - x_0)$  with the non-symmetric shift  $x_0 \neq 0$ . We find  $K_n = x_0^n/n!$  and the convergence condition reads  $x_0 < (n+1)/|k_m|$ . Subsequently, the Kuramoto-Sivashinsky equation is an approximation of (1) if  $x_0 < 2/|k_m|$  and if a maximum spatial frequency exists.

#### IV. LINEAR ANALYSIS

Now let us examine the stationary state and its linear behavior for a finite propagation speed  $c$ . In case of the stationary state  $V(x, t) = V_0$ , Eq. (1) recasts to

$$\begin{aligned} T(0)V_0 &= h(V_0) + \kappa_K f(V_0) + \kappa_L g(V_0), \\ \kappa_K &= \int_{-\infty}^{\infty} K(x)dx, \quad \kappa_L = \int_{-\infty}^{\infty} L(x)dx. \end{aligned} \quad (7)$$

with  $\kappa_K = \int K(x)dx$ ,  $\kappa_L = \int L(x)dx$ . Considering linear deviations  $u(x, t) = V(x, t) - V_0 \sim e^{\lambda t + ikx}$ , Eq. (1) reads

$$T(\lambda) = s_h + \int_{-\infty}^{\infty} dz M(z) e^{-\lambda|z|/c} e^{-ikz} \quad (8)$$

with  $M(z) = s_f K(z) + s_g L(z)$  and  $s_h = \delta h / \delta V$ ,  $s_f = \delta f / \delta V$ ,  $s_g = \delta g / \delta V$  computed at  $V = V_0$ , while  $\delta / \delta V$  denotes the functional derivative. In the following, the propagation delay  $c$  is assumed being large but finite and the approximation  $\exp(-\lambda|z|/c) \approx 1 - \lambda|z|/c + \lambda^2(|z|/c)$  holds. For the characteristic spatial scale of the system  $\sigma$ , we introduce the characteristic propagation delay  $\tau = \sigma/c$  which represents the delay time caused by the finite propagation speed. Thus the previous approximation holds for small propagation delays  $\tau \ll 1/\lambda$ . Subsequently expanding the exponential  $\exp(-ikz)$  into a power series we obtain

$$\begin{aligned} T(\lambda) &+ \frac{\lambda}{c} \sum_{n=0}^{\infty} (-ik)^n P_n - \frac{\lambda^2}{c^2} \sum_{n=0}^{\infty} (-ik)^n Q_n \\ &= s_h + \sum_{n=0}^{\infty} (-ik)^n M_n \end{aligned} \quad (9)$$

with the kernel moments  $M_n$  defined previously and  $P_n = \int_{\Omega} dz M(z) |z| z^n / n!$ ,  $Q_n = \int_{\Omega} dz M(z) |z|^2 z^n / n!$ . Preliminary computations of  $M_n$ ,  $P_n$  and  $Q_n$  for Gaussian kernels yield  $M_n \sim O(\sigma^n)$ ,  $P_n \sim O(\sigma^{n+1})$  and  $Q_n \sim O(\sigma^{n+2})$

Equation (9) defines the stability condition for general spatial interactions and short propagation delays. Additional more detailed studies show that large propagation speeds  $c$  with  $1/c^2 \approx 0$  and vanishing odd kernel moments  $M_{2n+1} = 0$ ,  $P_{2n+1} = 0$ ,  $Q_{2n+1} = 0$  lead to real Lyapunov exponents and thus may yield stationary bifurcations. In contrast oscillatory bifurcations may emerge for non-vanishing odd moments only. By recalling the definitions of these moments, we find that symmetric and non-symmetric spatial interactions may yield stationary and non-stationary bifurcations, respectively. In case of smaller propagation

speeds  $1/c^2 \neq 0$ , this classification does not hold anymore and oscillatory bifurcations may occur for both symmetric and non-symmetric kernels.

### A. The reaction-diffusion equation

To illustrate the latter results, first let us study a specific reaction-diffusion equation, namely the homogeneous diffusion equation also known as Ficks Second Law. According to the previous discussion, Eq. (3) represents the diffusion equation with  $\bar{h} = 0$  yielding  $h(V) = -f_1 V$ . Further Eq. (7) yields the stationary solution  $V_0 = 0$  and the parameters  $s_f = f_1$ ,  $s_h = -f_1$ , while the spatial interactions are given by  $K(z) \neq 0$  and  $L(z) = 0$ , i.e.  $M(z) = f_1 K(z)$ .

According to the previous discussion of (6), Eq. (2) represents a spatial mode expansion in orders of the characteristic spatial scale  $\sigma$ . That is, in the case of the diffusion equation, the order expansion is truncated at  $O(\sigma^3)$  yielding  $M_0 = f_1 \sim O(1)$ ,  $M_2 = f_1 \sigma^2/2 \sim O(\sigma^2)$  while all odd and higher kernel moments  $M_{2n}$  vanish with  $n \geq 2$ . Further we find  $P_0 = f_1 \sqrt{2\sigma}/\sqrt{\pi}$ ,  $P_1 = 0$ ,  $P_2 = f_1 \sqrt{2\sigma^3}/\sqrt{\pi}$  with  $P_n \approx 0 \forall n > 3$  and  $Q_0 = f_1 \sigma^2$ ,  $Q_n \approx 0 \forall n > 0$ . Here it is  $f_1 = 2D\sigma^2$  and  $D$  represents the diffusion constant. Subsequently in the case of  $c \rightarrow \infty$  Eq. (9) yields  $\lambda(k) \approx -Dk^2$  which is the well known dispersion relation of the diffusion equation. Figure 1 compares  $\lambda_{ex}$  and  $\lambda_{RD}$  and the corresponding resulting field activity for two values of  $\sigma$ . We observe that the IDE model is a good approximation to the diffusion equation for  $\sigma = 0.1$ , while the the approximation is much worse for  $\sigma = 2$ . This finding confirms our previous results on the convergence condition. Here the maximum value of  $|k|$  is  $2/\sigma$  according to the convergence condition  $\sigma < 2/k$  derived in the previous paragraphs.

Now let us turn to finite propagation speeds  $c < \infty$ . Considering the corresponding orders of  $M_n$ ,  $P_n$  and  $Q_n$ , Eq. (9) reads

$$\lambda + \frac{\lambda}{c}(P_0 - P_2 k^2) - \frac{\lambda^2}{c^2} Q_0 = s_h + M_0 - M_2 k^2. \quad (10)$$

For small propagation delays  $(\lambda\tau)^2 \rightarrow 0$  we find the Lyapunov exponent

$$\lambda_{RD}(k) = \frac{-Dk^2}{1 + \alpha\tau(1 - \sigma^2 k^2)} \quad (11)$$

with  $\alpha = f_1 \sqrt{2/\pi}$ . By virtue of the wavenumber limit  $|k| < 2/\sigma$ , there is a critical propagation delay  $\tau_{th} = 1/3\alpha$  and a corresponding critical propagation speed  $c_{th} = 3\alpha\sigma$ . Then small

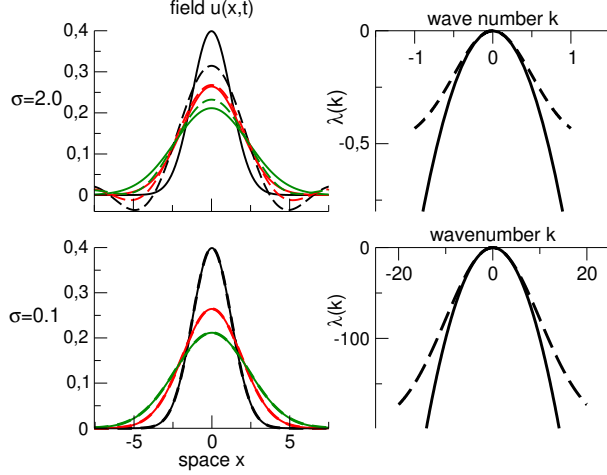


FIG. 1: (Color online) The field of the diffusion equation and the Lyapunov exponent for different spatial ranges  $\sigma$ . The dashed lines represent the results from the diffusion PDE, while the solid lines denote the results from the IDE model. In case of  $\sigma = 0.1$ , the reconstructed field  $u(x, t)$  obtained from the IDE can not be distinguished from the field of the original diffusion equation. In addition the colors in the left panel denote subsequent times  $t = 0$ (black),  $t = 3$ (red) and  $t = 6$ (green). That is the field  $u(x, t)$  flattens at increasing time.

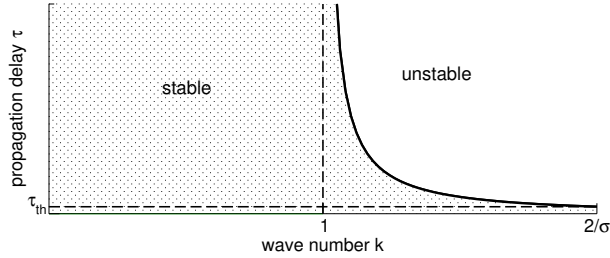


FIG. 2: Illustrated stability diagram of the extended diffusion equation. The vertical axis  $k = 1$  represents the asymptote of the instability regime.

delays  $\tau < \tau_{th}$  retain the field stability, while large delays  $\tau > \tau_{th}$  yield linear unstable modes  $k$  with  $\lambda_{RD}(k) > 0$ . Figure 2 shows the corresponding stability diagram of the system.

Moreover, Eq. (11) may be interpreted as if it originates from the modified diffusion equation

$$\frac{\partial u(x, t)}{\partial t} + \frac{\alpha\sigma}{c} \left( 1 + \sigma^2 \frac{\partial^2}{\partial x^2} \right) \frac{\partial u(x, t)}{\partial t} = D \frac{\partial^2 u(x, t)}{\partial x^2} \quad (12)$$

To our best knowledge, this equation represents an extension of diffusion equations considering finite propagation speeds. It applies in media whose propagation delay on the typical

length scale of the system is not negligible and, for instance, which show delayed spread of space-time activity. We mention results from fast hot pulses in plasma [36], whose investigation indicates nonlocal effects in the reaction-diffusion mechanism. Moreover, there is the debate on the non-Fourier heat conduction in nonhomogeneous materials which show such delayed temporal activity at measurement points [8, 9, 39]. In order to compare our model to the results found in experiments [9], Fig. 3 shows the temporal activity at a spatial point. We observe a dramatic delay of the activity at large delays, while  $\tau \rightarrow 0$  yields the Fourier case. This finding is irrespective of the spatial location used and coincides qualitatively to experimental findings. Moreover, the derived model (12) contrasts to the Cattaneo equation [12, 40], which represents a telegraphic equation and extends the parabolic diffusion equation to a hyperbolic partial differential equation by an additional second temporal derivative and thus involves finite propagation speed. Originally the Cattaneo extension has been proposed according to heuristic arguments while our model is derived from the explicit treatment of propagation delay.

At last, let us briefly focus on the case of larger propagation delays  $(\lambda\tau)^3 \rightarrow 0$  yielding the implicit equation  $-\lambda^2\tau^22D/\sigma^2 + \lambda(1 + \alpha D\tau(1 - \sigma^2k^2)) - Dk^2 = 0$ . Simple calculus reveals  $Re(\lambda) > 0$  for some  $k$  and larger delays destabilize the field similar to the previous case of small delays.

## B. The Swift-Hohenberg equation

Now let us turn to the Swift-Hohenberg model which involves long-range spatial interactions. The stationary state is given by Eq. (7) and we find one or three solutions. The

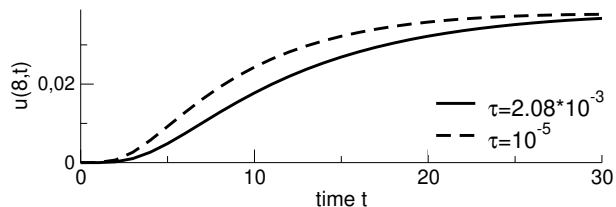


FIG. 3: Temporal activity of the modified diffusion equation at spatial location  $x = 8$  for two different propagation delays, i.e. propagation speeds. The solutions are computed analytically with initial condition  $u(k, t = 0) = \exp(-k^2/2 \cdot 0.8^2)/\sqrt{2\pi 0.8^2}$ .

single solution  $V_0 = 0$  leads to the parameters  $s_f = -|f_1|$  and  $s_h = a$ . Further the spatial interactions are given by  $K(z) \neq 0$  and  $L(z) = 0$  yielding  $M(z) = -|f_1|K(z)$ .

According to the discussions in section III D, Eq. (2) breaks off at order  $O(\sigma^5)$  and we obtain the expansion terms

$$\begin{aligned} M_0 &= -|f_1|, \quad M_2 = -|f_1|\sigma^2/2, \quad M_4 = -|f_1|\sigma^4/8 \\ P_0 &= -|f_1|\sqrt{\frac{2}{\pi}}\sigma, \quad P_2 = -|f_1|\sqrt{\frac{2}{\pi}}\sigma^3, \quad P_4 = -|f_1|\frac{\sqrt{2}}{3\sqrt{\pi}}\sigma^5 \\ Q_0 &= -|f_1|\sigma^2, \quad Q_2 = -|f_1|\frac{3}{2}\sigma^4 \end{aligned}$$

while all odd and higher terms  $M_n$ ,  $P_n$ ,  $Q_n$  vanish. Subsequently Eq. (9) yields for  $c \rightarrow \infty$

$$\lambda_\infty = \frac{|f_1|}{2} (\epsilon - 1 + 2l^2 - l^4)$$

with the scaled wavenumber  $l = \sigma k / \sqrt{2}$  and  $\epsilon$  taken from section III B. Here  $\lambda_\infty$  represents the Lyapunov exponent of the linearized original Swift-Hohenberg equation (4) and thus defines the linear stability of the underlying spatial system. To be more detailed, for  $\epsilon < 0$  the system is linear stable with  $\lambda_\infty < 0$  for all  $l$ , while  $\epsilon > 0$  yields  $\lambda_\infty > 0$  for  $1 - \sqrt{\epsilon} < l < 1 + \sqrt{\epsilon}$ . In other words, a Turing instability emerges for  $\epsilon > 0$  at scaled wavenumbers  $|l| \approx 1$ .

Now let us turn to the case  $c < \infty$ . For small propagation delays  $(\lambda\tau)^2 \rightarrow 0$  we find

$$\lambda_{SH} = \frac{\lambda_\infty}{1 - \alpha(1 - 2l^2 + 4l^4/3)\tau} \quad (13)$$

with  $\alpha = |f_1|\sqrt{2/\pi}$ . Here  $\lambda_{SH}$  represents the Lyapunov exponent of the Swift-Hohenberg equation subject to large propagation speeds. It is important to mention that the validity criteria  $0 < \sigma^2 < 6/k_m^2$  derived in section III D delimits the scaled wavenumber to  $-\sqrt{3} < l < \sqrt{3}$ . Taking into account this constraint, closer examinations of Eq. (13) reveal the critical propagation delay  $\tau_{th} = 1/7\alpha$  and the corresponding critical propagation speed  $c_{th} = 7\alpha\sigma$ . For  $\tau < \tau_{th}$ , the denominator of  $\lambda_{SH}$  is positive for all valid wavenumbers and thus  $\lambda_\infty$  defines the stability of the system. Hence the propagation delay does not affect the stability of the system.

In contrast large propagation delays  $\tau > \tau_{th}$  yield a negative denominator for a half-band of wavenumbers  $|l| > l_{th}$  and thus change the sign of the Lyapunov exponent. Here the critical wavenumber  $l_{th}$  represents the root of the denominator in Eq. (13). Figure 4 shows the stability diagram of Eq. (13). We observe the unstable half-band for  $\tau > \tau_{th}$  for all  $\epsilon$ , while

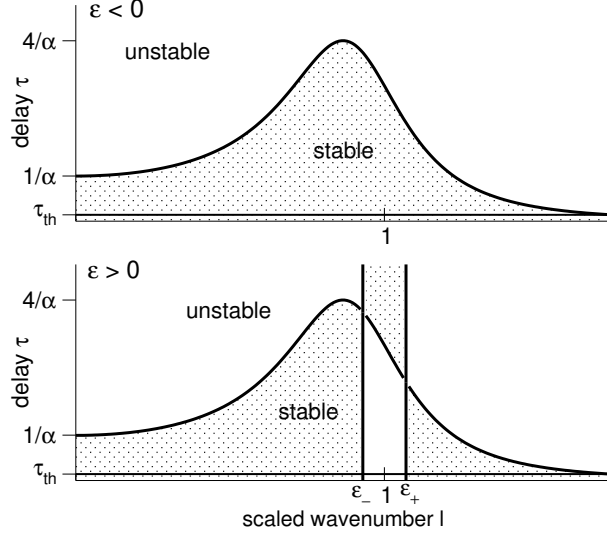


FIG. 4: Illustrated stability diagram of the extended Swift-Hohenberg equation involving propagation delays. For  $\varepsilon < 0$  (top panel) the underlying system is stable for  $\tau < 1/\alpha(1 - 2l^2 + 4l^4/3)$  and unstable otherwise. For  $\varepsilon > 0$  (bottom panel) the stability is the same as for  $\varepsilon < 0$  besides the wavenumber band  $\varepsilon_- < l < \varepsilon_+$ ,  $\varepsilon_{\pm} = \pm\sqrt{\varepsilon}$ . For short delays  $\tau < 1/\alpha(1 - 2l^2 + 4l^4/3)$  the underlying system is linear unstable in this wavenumber band, while the modes in this band are stable otherwise. In both latter cases  $\tau < \tau_{th}$  guarantees the linear stability of the underlying system.

$\tau > 1/\alpha > \tau_{th}$  yields an additional unstable band of wavenumbers around  $l = 0$ . For  $\varepsilon < 0$  the stable band of spatial modes vanish for large propagation delays  $\tau > 4/\alpha$  and the system is totally destabilized, while for  $\varepsilon > 0$  increased propagation delays stabilize the band of unstable Turing-modes. This stabilization by propagation delays represents a new kind of space-time dynamics near Turing instabilities. In addition recall that the previous treatment around  $l_{th}$  reflects  $|\lambda| \rightarrow \infty$  and thus conflicts with the previous assumption  $(\lambda\tau)^2 \approx 0$ . Subsequently higher polynomial orders in  $\lambda$  are necessary for closer examinations.

Finally Eq. (13) may be interpreted as if it originates from the extended Swift-Hohenberg equation

$$\begin{aligned} \frac{\partial V(x, t)}{\partial t} - \frac{\alpha\sigma}{c} \left( 1 + 2\frac{\partial^2}{\partial x^2} + \frac{4}{3}\frac{\partial^4}{\partial x^4} \right) \frac{\partial V(x, t)}{\partial t} \\ = \epsilon V(x, t) - V^3(x, t) - \left( 1 + \frac{\partial^2}{\partial x^2} \right)^2 V(x, t) \end{aligned} \quad (14)$$

with the re-scaled time  $t \rightarrow 2t/|f_1|$ . To our best knowledge, this equation represents an extension of the Swift-Hohenberg equation involving a finite propagation speed. In the case of a infinite propagation speed  $c \rightarrow \infty$  the additional second term on the left hand side of Eq. (14) vanishes and the original model equation is re-gained. Further the finite propagation speed leads to the coupling term between spatial and temporal derivatives in Eq. (14) reflecting the space-dependant delay in Eq. (1).

### C. The Kuramoto-Sivashinsky equation

Finally let us investigate the Kuramoto-Sivashinsky equation by following the same steps as in the previous examples. Now Eq. (9) reads for small propagation delays  $(\lambda\tau)^2 \approx 0$

$$\lambda + \frac{\lambda}{c}(P_0 - k^2 P_2) = s_h + M_0 - ikM_1 - k^2 M_2 + k^4 Q_2.$$

with  $M_0 = s_f + s_g$ ,  $M_1 = s_f x_0$ ,  $M_2 = s_g \sigma^2/2$ ,  $M_4 = s_g \sigma^4/8$ ,  $P_0 = s_f x_0 + s_g \sqrt{2}\sigma/\sqrt{\pi}$ ,  $P_2 = s_g \sqrt{2}\sigma^3/\sqrt{\pi}$  and  $M_n$ ,  $P_m \rightarrow 0$  for  $n > 4$ ,  $m > 2$ . The stationary solution is taken from (7) and reads  $V_0 = 0$  yielding  $s_f = 0$ ,  $s_g = g_1$  and the Lyapunov exponent

$$\lambda_{KS} = \frac{-\eta + l^2 - l^4}{1 - \tau\alpha(1 - 4l^2)} \quad (15)$$

with  $\alpha = |g_1|\sqrt{2/\pi}$ ,  $l = \sigma k/2$  and  $\lambda_{KS} = \lambda/2|g_1|$ . We point out that the re-scalings  $k \rightarrow l$  and  $\lambda \rightarrow \lambda_{KS}$  are identical to the re-scalings of space and time in section III C.

Now let us examine (15) in some more detail. For a vanishing propagation delay  $\tau = 0$   $\lambda_{KS}$  becomes the Lyapunov exponent well-known for the original Kuramoto-Sivashinsky model. This means the stationary solution is linear unstable at wavenumbers  $-1 < l < 1$  while it

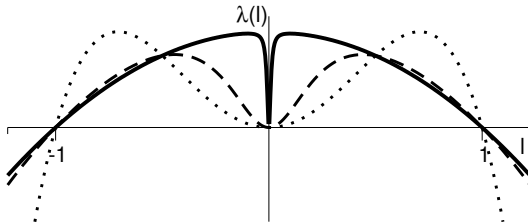


FIG. 5: The Lyapunov exponent of the Kuramoto-Sivashinsky equation subject to the scaled wave number  $l$ . The different line styles encode the different propagation delays  $\tau = 0$  (dotted line),  $\tau = 2.0$  (dashed line) and  $\tau = 2.499$  (solid line). It is  $\tau_{th} = 2.5$ .

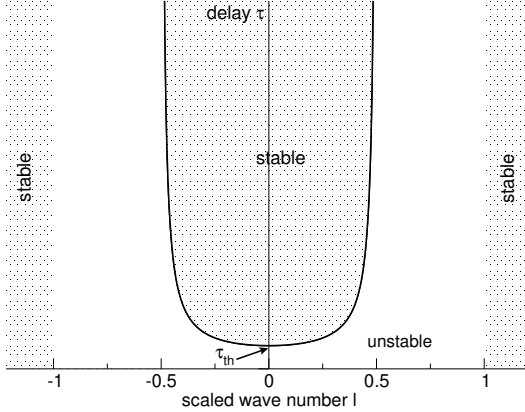


FIG. 6: The illustrated stability diagram of the extended Kuramoto-Sivashinsky equation subject. The center stability region does not exceed the interval  $[-0.5, 0.5]$  on the horizontal axis.

is linear stable otherwise. In case of  $\tau \neq 0$ , the propagation delay changes the Lyapunov exponent and may destabilize the system. It turns out that there is a critical propagation delay  $\tau_{th} = 1/\alpha$  and a corresponding a critical propagation speed  $c_{th} = \alpha\sigma$ . For small propagation delays  $\tau < \tau_{th}$ , the Lyapunov exponents are modified but the system stability is retained, see Fig. 5). In contrast large propagation delays  $\tau > \tau_{th}$  lead to a sign inversion of the Lyapunov exponent for  $-l_c < l < l_c$  with  $l_c^2 = 1 - 1/\alpha\tau$ . Figure 6 summarizes the stability conditions in a diagram. However  $\tau \rightarrow \tau_{th}$  yields  $\lambda \rightarrow \infty$  for  $l \rightarrow l_c$  and thus does not fulfill the previous condition  $(\lambda\tau)^2 \approx 0$ .

Finally, Eq. (15) may be interpreted as if it originates from the PDE

$$\begin{aligned} \frac{\partial V(x, t)}{\partial t} - \frac{\sigma\alpha}{c} \left( 1 + 4 \frac{\partial^2}{\partial x^2} \right) \frac{\partial V(x, t)}{\partial t} = \\ -\eta V - \frac{\partial^2}{\partial x^2} V(x, t) - \frac{\partial^4}{\partial x^4} V(x, t) - V \frac{\partial V}{\partial x} \end{aligned} \quad (16)$$

This equation represents an extension of the Kuramoto-Sivashinsky equation now involving large propagation speeds  $c$ . We observe that  $c \rightarrow \infty$  yields the original Kuramoto-Sivashinsky equation, while the finite propagation speed leads to the additional second term on the left hand side.

## V. CONCLUSION

The present work has introduced a nonlocal integral-differential equation model which generalizes three important partial differential equations. Moreover we have shown how

to consider large propagation speeds in these models and have quantified the propagation delay as the fraction of spatial interaction range and propagation speed. The subsequent linear stability analysis turns out to be dependent on this quantity and reveals critical propagation delays and corresponding propagation speeds. We find that large propagation speeds slow down the activity spread in diffusion systems and thus allows for the explanation of non-Fourier behavior in non-homogeneous systems. Further finite propagation speeds may destabilize the dynamics of Swift-Hohenberg equation in the stable regime of the original equation, while it may stabilize an occurring Turing instability. Finally finite propagation speeds may stabilize the dynamics of the Kuramoto-Sivashinsky equation. For all three models novel partial differential equations have been formulated which incorporate the propagation delay effects. We are convinced that propagation delays play an important role in media showing ultra-fast phenomena and that the obtained results shall allow for their modeling.

## VI. ACKNOWLEDGMENT

The author thanks R.Metzler for interesting discussions and acknowledges the financial support from the Deutsche Forschungsgemeinschaft (grant Sfb-555).

---

- [1] S. Coombes, *Biological Cybernetics* **93**, 91 (2005).
- [2] H. Haken, *Synergetics: Introduction and Advanced topics* (Springer, Berlin, 2004).
- [3] H. Haken, *Brain Dynamics* (Springer, Berlin, 2002).
- [4] C.Eurich, M.C.Mackey, and H.Schwegler, *J. Theor. Biol.* **216**, 31 (2002).
- [5] C. Laing and S. Coombes, *Network: Computation in Neural Systems* **17**, 151 (2006).
- [6] A.Hutt and T.D.Frank, *Acta Physica Polonica A* **108**, 1021 (2005).
- [7] Th.Martin and R.Landauer, *Phys. Rev. A* **45**, 2611 (1992).
- [8] D.Y.Tzou and J.K.Chen, *J. Thermophys. Heat Transfer* **12**, 567 (1998).
- [9] K.Mitra, S.Kumar, A.Vedavarz, and M.K.Moallemi, *ASME J. Heat Transfer* **117**, 568 (1995).
- [10] T.Weller and B.Hajek, *IEEE/ACM Trans. Networking* **5**, 813 (1997).
- [11] I.E.Pountourakis, *Information Sciences Informatics and Computer Science* **157**, 111 (2003).

- [12] C. Cattaneo, *Comptes Rendus* **247**, 431 (1958).
- [13] L.Glass and M.C.Mackey, *From Clocks to Chaos: The Rhythms of Life* (Princeton University Press, Princeton, 1988).
- [14] W. Gerstner, *Phys. Rev. E* **51**, 738 (1995).
- [15] S.M.Crook, G.B.Ermentrout, M.C.Vanier, and J.M.Bower, *J. Comput. Neurosci.* **4**, 161 (1997).
- [16] J.D.Murray, *Mathematical Biology* (Springer, Berlin, 1989).
- [17] L.D.Landau and E.M.Lifshitz, *Fluid Mechanics* (Butterworth-Heinemann, Boston, 1987).
- [18] M. Walgraef, *Spatio-Temporal Pattern Formation* (Springer, New York, 1996).
- [19] G. Nicolis and I. Prigogine, *Self-Organization in Non-Equilibrium Systems: From Dissipative Structures to Order Through Fluctuations* (J. Wiley and Sons, New York, 1977).
- [20] M.C.Cross and P.C.Hohenberg, *Reviews of Modern Physics* **65**, 851 (1993).
- [21] J.B.Swift and P.C.Hohenberg, *Phys. Rev. A* **15**, 319 (1977).
- [22] J.Lega, J.V.Moloney, and A.C.Newell, *Phys.Rev.Lett.* **73**, 2978 (1994).
- [23] S.Longhi and A.Geraci, *Phys. Rev. A* **54**, 4581 (1996).
- [24] J.M.Hyman, B.Nicolaenko, and S.Zaleski, *Physica D* **23**, 265 (1986).
- [25] B.I.Shraiman, *Phys. Rev. Lett.* **57**, 325 (1986).
- [26] U.Frisch, Z.S.She, and O.Thual, *J. Fluid Mechn.* **186**, 221 (1986).
- [27] A.Novick-Cohen, *Physica D* **26**, 403 (1987).
- [28] R. Friedrich, G. Radons, T. Ditzinger, and A. Henning, *Phys. Rev. Lett.* **85**, 4884 (2000).
- [29] A.Hutt and F.M.Atay, *Physica D* **203**, 30 (2005).
- [30] F. M. Atay and A. Hutt, *SIAM J. Appl. Math.* **65**, 644 (2005).
- [31] G.B.Ermentrout, *Reports on Progress in Physics* **61**, 353 (1998).
- [32] V.K.Jirsa, *Neuroinformatics* **2**, 183 (2004).
- [33] P.C.Bressloff and S.Coombes, *Int. J. Mod. Phys. B* **11**, 2343 (1997).
- [34] M.Fujimoto, S.Aoshima, M.Hosoda, and Y.Tsuchiya, *Optics Letters* **24**, 850 (1999).
- [35] G.W.Rieger, K.S.Virk, and J.F.Young, *Appl. Phys. Lett.* **84**, 900 (2004).
- [36] E.Lazzaro and H.Wilhelmsson, *Physics of plasmas* **5**, 2830 (1998).
- [37] U.Bovensiepen, *Appl. Phys. A* **82**, 395 (2006).
- [38] I.N.Aliev, *Technical Physics Letters* **21**, 126 (1995).
- [39] H.Herwig and K.Beckert, *Heat and Mass Transfer* **36**, 387 (2000).

[40] R.Metzler and T.F.Nonnenmacher, Phys.Rev.E **57**, 6409 (1998).